Energy & Environmental Science

Cite this: DOI: 10.1039/c2ee21437g

www.rsc.org/ees

COMMUNICATION

# Improving the cycling stability of silicon nanowire anodes with conducting polymer coatings†

Yan Yao,[a] Nian Liu,[b] Matthew T. McDowell,[a] Mauro Pasta[a] and Yi Cui*[ac]

*Received 21st February 2012, Accepted 24th April 2012*
**DOI: 10.1039/c2ee21437g**



**For silicon nanowires (Si NWs) to be used as a successful high capacity lithium-ion battery anode material, improvements in cycling stability are required. Here we show that a conductive polymer surface coating on the Si NWs improves cycling stability; coating with PEDOT causes the capacity retention after 100 charge–discharge cycles to increase from 30% to 80% over bare NWs. The improvement in cycling stability is attributed to the conductive coating maintaining the mechanical integrity of the cycled Si material, along with preserving electrical connections between NWs that would otherwise have become electrically isolated during volume changes.**

Rechargeable lithium-ion batteries have been identified as the most promising energy storage technology for portable electronics and electric vehicles.[1,2] Novel materials and chemistries are being developed to improve energy density and cycling stability, which are the two most important criteria for the target applications.[3–6] Alloying anode materials, such as Si, Sn, Ge, and Al, have attracted significant interest due to their high theoretical Li storage capacity.[7–9] However, large volume changes of up to 400% during (de)lithiation of alloying anodes lead to significant mechanical stress and can cause fracture of the electrode, severely limiting practical applications.[10,11] Nanostructuring of these materials has been found to successfully alleviate (de)lithiation-induced stress; for example, several groups have demonstrated good electrochemical performance of Si nanostructured anodes.[12–15] Although significant progress has been made in improving Si nanostructure-based anodes, further improvements in cycling stability are urgently required to make them commercially viable.

Conductive polymers are an important class of materials with various applications in electronics,[16] optics,[17,18] batteries,[19] and supercapacitors.[20,21] Compared to the commonly used method of carbon coating of battery electrodes, which requires a high temperature (above 700 °C) pyrolysis process,[22] conductive polymer coatings can be applied at low temperature and are scalable. Conductive polymer coatings for battery cathode materials have been quite successful.[23,24] For example, an excellent rate performance (10*C*) has been demonstrated for polypyrrole-coated $LiFePO_4$ particles without any carbon additives.[23] However, only a limited number of examples have been reported for anode materials. Recently, Lee and Jung showed that Ag/poly(3,4-ethylenedioxythiophene) (PEDOT) nanocomposites showed good electrochemical behavior as an anode.[25]

In this communication, we report that conductive polymer coatings improve the cycling stability of Si NW electrodes in Li ion batteries. PEDOT is used due to its high electrical conductivity and good electrochemical stability. The conductivity of PEDOT at negative voltage (n-doped state) is around 0.1 S $cm^{-1}$,[26] and PEDOT can be directly deposited onto the surface of Si NWs by electropolymerization. Our experiments show that 2500 mA h $g^{-1}$ (80% of the initial capacity) is retained after 100 cycles for PEDOT-coated Si NWs compared to 30% in the case of pristine Si NWs under the same cycling conditions.

The electrochemical polymerization and simultaneous deposition of PEDOT coatings onto Si NWs were performed in a glass cell using 0.01 M 3,4-ethylenedioxythiophene (EDOT) as the monomer in a $LiClO_4$/EtCN electrolyte. Si NWs were grown by Au-catalyzed

[a]*Department of Materials Science and Engineering, Stanford University, Stanford, California, 94305, USA. E-mail: yicui@stanford.edu*
[b]*Department of Chemistry, Stanford University, Stanford, California, 94305, USA*
[c]*Stanford Institute for Materials and Energy Sciences, SLAC National Accelerator Laboratory, 2575 Sand Hill Road, Menlo Park, California 94025, USA*

† Electronic supplementary information (ESI) available: Additional experimental details and figures. See DOI: 10.1039/c2ee21437g

## Broader context

Silicon nanowires are promising high capacity anode materials for next generation lithium-ion batteries. We show that a conductive polymer coating can significantly increase the capacity retention with cycling. The polymer coating was applied *via* an electrochemical polymerization process, and the resulting polymer–Si hybrid nanostructures were characterized with electron microscopy and X-ray photoelectron spectroscopy. This organic–inorganic hybrid approach represents a facile method for improving the performance of alloying anodes for Li-ion batteries.

chemical vapor deposition and were used as the working electrode. The electropolymerization was conducted galvanostatically (1 mA $cm^{-2}$), limiting the charge at 120 mC $cm^{-2}$. In general, electropolymerization processes involve generation of cation radicals and coupling of the radicals for chain growth. The oxidation potential of EDOT has been reported to be 1.25 V *vs.* Ag/AgCl (3.5 M) in the literature,[27] and a similar potential of 1.3 V *vs.* Ag/AgCl was observed in our experiments during galvanostatic electropolymerization (Fig. S1†). Upon polymerization, the color of the Si NWs changed from brown to blue, indicating the formation of the PEDOT coating layer. Fig. 1 shows SEM images of Si NWs before (A) and after (B) PEDOT coating. Each individual Si NW was coated uniformly along the entire length. The magnified SEM image in Fig. 1C shows the granular and porous structure of PEDOT, with granule sizes in the range of ~50 nm. This granular morphology is common for electrochemically polymerized polymers due to heterogeneous nucleation on the Si NW surfaces.[23] Transmission electron microscopy (TEM) was used to examine the morphology of an individual coated Si NW, revealing the size of the Si NW and the thickness of the coating. In Fig. 1E, the full width of the PEDOT-coated Si NW is observed to be ~300 nm, and the PEDOT layer is ~100 nm thick. An energy dispersive X-ray spectroscopy (EDX) line scan confirms these observations, with a silicon signal coming from the core and a sulfur signal coming from the PEDOT layer. X-ray photoelectron spectroscopy (XPS) was also used to characterize the PEDOT coating layer on the Si NWs. Pristine Si NWs exhibit Si (2s) and Si (2p) peaks, as shown in Fig. 2A. The O (1s) peak may come from native silicon oxide on the NWs. Fig. 2B shows C (1s), S (2s), S (2p), and O (1s) peaks, which are characteristic peaks of PEDOT. The Cl (2p) peak comes from the dopant of $ClO_4^-$ in PEDOT, which is a remnant of the $LiClO_4$ salt used during electrochemical polymerization. The Si (2s) or Si (2p) signals are not detected, which proves that all the Si NW surfaces are completely covered with PEDOT because the depth sensitivity of XPS is around 10 nm. Taken together, the XPS, SEM and TEM results show that the electrochemically polymerized PEDOT uniformly covers the high-aspect SiNW array.

To study the electrochemical properties of PEDOT-coated Si NWs, cyclic voltammetry (CV) was performed at a scan rate of 0.1 mV $s^{-1}$ over the potential window of 0.01–1 V *vs.* $Li/Li^+$. Standard coin cells (2032) were made using lithium foil as the counter electrode and Celgard 2250 as the separator. The electrolyte was 1.0 M $LiPF_6$ in 1 : 1 w/w ethylene carbonate: diethyl carbonate (Novolyte Technologies). As shown in Fig. 3A, the second cycle of the CV profile of PEDOT-coated Si NWs exhibits similar characteristics to that of the pristine Si NWs. In the cathodic branch, the peak at 0.19 V corresponds to the conversion of a-Si to the $Li_xSi$ phase. The two peaks at 0.41 and 0.55 V in the anodic branch correspond to delithiation of a-$Li_xSi$ to a-Si. The black line in the same figure shows the second cycle CV profile of pristine Si NWs; the redox peaks are present at similar positions, although the amplitude is slightly smaller. The CV scan of a pure PEDOT film is also shown (blue curve). The current density is two orders of magnitude smaller than that of the PEDOT-coated Si, indicating the negligible contribution from PEDOT to the capacity of the whole electrode. Fig. S2† shows a galvanostatic voltage profile for a pure PEDOT film deposited on a Pt electrode as a control experiment. In this case, the pure PEDOT film exhibited

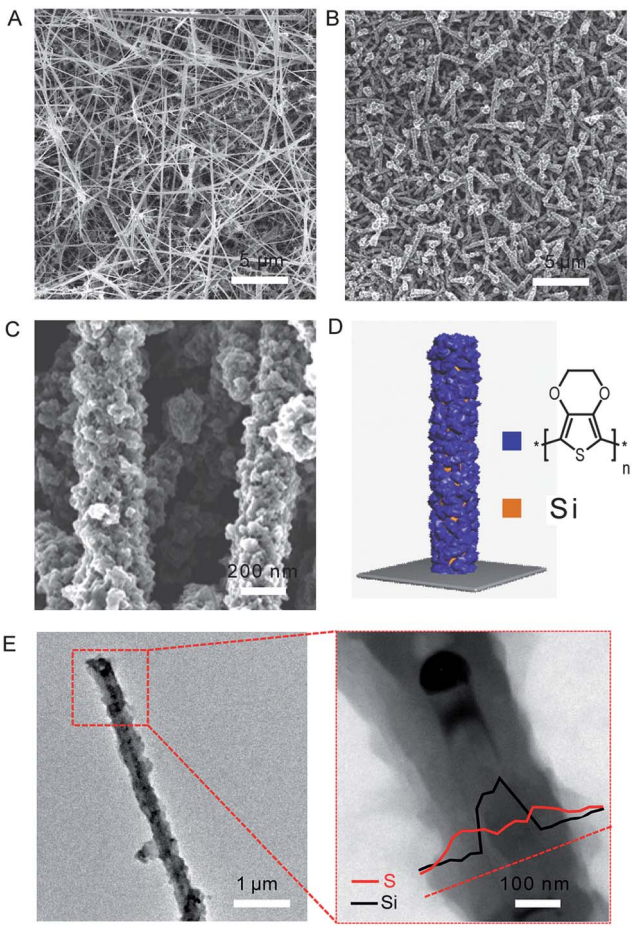


**Fig. 1** (A and B) Top view SEM images of pristine Si NWs and PEDOT-coated Si NWs. Scale bar: 5 μm. (C) Magnified SEM image of PEDOT-coated Si NWs. (D) Schematic of a PEDOT (blue)-coated Si NW (brown) with the molecular structure of PEDOT shown. (E) TEM images of an individual PEDOT-coated Si NW. The EDX line scan profile shows the sulfur signal from PEDOT (red) and the Si signal from the core (black).

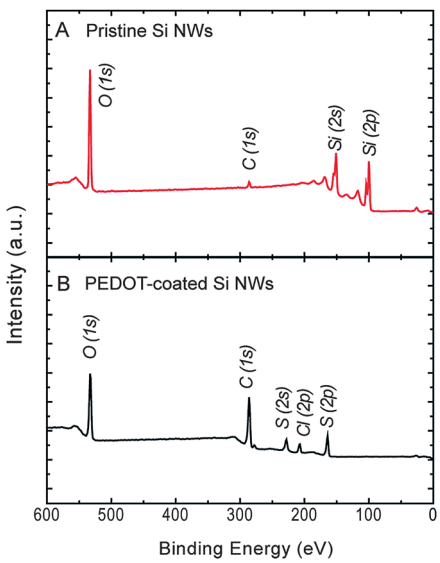


**Fig. 2** XPS characterization of PEDOT-coated Si NWs. (A) Pristine Si NW sample, (B) PEDOT-coated Si NW sample. The S signal is from PEDOT. No Si peaks were observed, which indicates the uniform and complete coverage of PEDOT on the Si NWs.

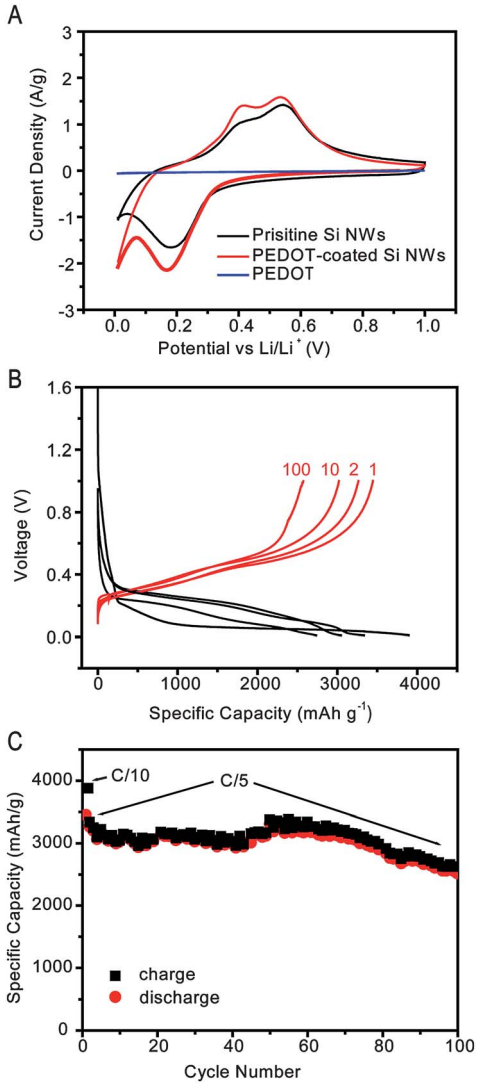


**Fig. 3** Electrochemical characterization of PEDOT-coated Si NW anodes. (A) Cyclic voltammetry (2nd cycle) of pristine Si NWs, PEDOT-coated Si NWs and a pure PEDOT electrode. (B) Galvanostatic charge–discharge voltage profile of PEDOT-coated Si NWs for the 1st, 2nd, 10th and 100th cycle. (C) Specific capacity with cycling of PEDOT-coated Si NWs. The first cycle is at *C*/10 and the remaining cycles are at *C*/5 ($1C$ = 4200 mA $g^{-1}$).

a specific capacity of 100 mA h $g^{-1}$ in the voltage range of 0.01–2 V *vs.* $Li/Li^+$.

Fig. 3B shows the voltage profiles for the 1st, 2nd, 10th, and 100th galvanostatic charge–discharge cycles. For the first cycle at a rate of *C*/10 (0.42 A $g^{-1}$; $1C$ denotes charging the electrode in one hour), the charge and discharge capacities reach 3850 and 3445 mA h $g^{-1}$. The capacity is calculated based on Si mass only, which accounts for 90% of the total mass. The Coulombic efficiency (CE) for the first cycle is 89%, which is similar to that of bare Si NWs (Fig. S3†). The second and later cycles were performed at a rate of *C*/5 (0.84 A $g^{-1}$), and the charge/discharge capacity *versus* cycle number is shown in Fig. 3C. The discharge capacities for the 2nd and 100th cycles are 3263 and 2510 mA h $g^{-1}$, respectively. This corresponds to an average capacity decay of 0.23% per cycle. The capacity decays faster in the last 30 cycles, but overall 80% capacity is retained after 100 cycles for

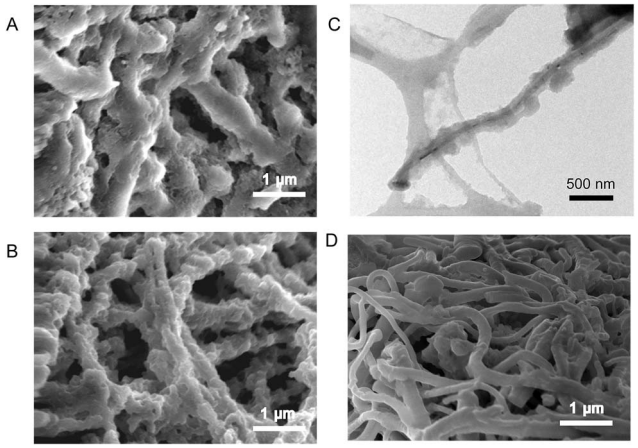


**Fig. 4** Characterization of Si NW anodes after 40 charge–discharge cycles. (A) SEM image of PEDOT-coated Si NW anode with SEI. (B) SEM and (C) TEM image of PEDOT-coated Si NW anode with SEI removed by dipping in 0.5 M HCl, showing that the PEDOT coating remains on the surface of the Si NWs. (D) SEM image of non-coated Si NW anode with SEI removed.

PEDOT-coated Si NW anodes. In comparison, data from pristine Si NW anodes cycled under the same conditions are shown in Fig. S3†, showing only 30% capacity retention after 100 cycles.

One key failure mechanism for cycling stability in Si NWs is fracture and pore formation during repeated lithiation/delithiation cycles,[28–30] which can lead to a loss of active material. With this in mind, we hypothesize that the PEDOT coating could improve capacity retention by mechanically and electrically binding the porous $Si/Li_xSi$ structure together during lithiation/delithiation. To test this hypothesis, cells were opened in a glove box after 40 charge/discharge cycles, and the morphology of the anodes was studied with SEM and TEM. Fig. 4 shows the morphology before and after removal of the SEI. The SEI layer is clearly seen in Fig. 4A. When removed with HCl, the PEDOT coating remains as seen in Fig. 4B and C: the PEDOT coating remains uniform even after many charge and discharge cycles. In contrast, we observed some cracks in non-coated Si NWs after the same number of cycles in Fig. 4D. This indicates that the coating could act to maintain the mechanical integrity of the cycled Si material, along with preserving electrical connections between NWs that would otherwise have become electrically isolated during volume changes. In addition, since the PEDOT is exposed to the electrolyte instead of Si, the nature of the SEI-forming side reactions could be different during electrochemical cycling, and this could contribute to the improved capacity retention.

## Conclusions

We have demonstrated that conductive PEDOT coatings on Si NWs lead to a notable improvement of the cycling performance of Si NW anodes. During prolonged cycling, the capacity retention after coating with PEDOT increases from 30% to 80% over 100 cycles. This organic–inorganic hybrid material presents a promising direction for improving the performance of lithium ion batteries.

## Acknowledgements

This work was partially supported by the Assistant Secretary for Energy Efficiency and Renewable Energy, Office of Vehicle

Technologies of the U.S. Department of Energy under contract no. DE-AC02-05CH11231, subcontract no. 6951379 under the Batteries for Advanced Transportation Technologies (BATT) Program. Y.C. acknowledges support from the King Abdullah University of Science and Technology (KAUST) Investigator Award (no. KUS-l1-001-12). A portion of this work is also supported by the Department of Energy, Office of Basic Energy Sciences, Division of Materials Sciences and Engineering, under contract DE-AC02-76SF0051, through the SLAC National Accelerator Laboratory LDRD project. M.T.M. acknowledges support from the Chevron Stanford Graduate Fellowship, the National Defense Science and Engineering Graduate Fellowship, and the National Science Foundation Graduate Fellowship.



## Notes and references

1 J. M. Tarascon and M. Armand, *Nature*, 2001, **414**, 359–367.
2 P. G. Bruce, B. Scrosati and J.-M. Tarascon, *Angew. Chem., Int. Ed.*, 2008, **47**, 2930–2946.
3 E. J. Cairns and P. Albertus, *Annu. Rev. Chem. Biomol. Eng.*, 2010, **1**, 299–320.
4 R. Malik, F. Zhou and G. Ceder, *Nat. Mater.*, 2011, **10**, 587–590.
5 X. Ji, S. Evers, R. Black and L. F. Nazar, *Nat. Commun.*, 2011, **2**, 325.
6 G. Girishkumar, B. McCloskey, A. C. Luntz, S. Swanson and W. Wilcke, *J. Phys. Chem. Lett.*, 2010, **1**, 2193–2203.
7 N. S. Choi, Y. Yao, Y. Cui and J. Cho, *J. Mater. Chem.*, 2011, **21**, 9825.
8 M. N. Obrovac and L. J. Krause, *J. Electrochem. Soc.*, 2007, **154**, A103.
9 H. Kim, M. Seo, M.-h. Park and J. Cho, *Angew. Chem., Int. Ed.*, 2010, **49**, 2146–2149.
10 R. A. Huggins, *J. Power Sources*, 1999, **81–82**, 13–19.
11 L. Y. Beaulieu, K. W. Eberman, R. L. Turner, L. J. Krause and J. R. Dahn, *Electrochem. Solid-State Lett.*, 2001, **4**, A137.
12 C. K. Chan, H. Peng, G. A. O. Liu, K. Mcilwrath, X. F. Zhang, R. A. Huggins and Y. Cui, *Nat. Nanotechnol.*, 2008, **3**, 31–35.
13 M. H. Park, K. Kim, J. Kim and J. Cho, *Adv. Mater.*, 2010, **22**, 415–418.
14 Y. Yao, M. T. McDowell, I. Ryu, H. Wu, N. Liu, L. Hu, W. D. Nix and Y. Cui, *Nano Lett.*, 2011, **11**, 2949–2954.
15 A. Magasinski, P. Dixon, B. Hertzberg, A. Kvit, J. Ayala and G. Yushin, *Nat. Mater.*, 2010, **9**, 353–358.
16 M. A. Bangar, W. Chen, N. V. Myung and A. Mulchandani, *Thin Solid Films*, 2010, **519**, 964–973.
17 C. M. Hangarter, M. Bangar, A. Mulchandani and N. V. Myung, *J. Mater. Chem.*, 2010, **20**, 3131.
18 P. M. Beaujuge and J. R. Reynolds, *Chem. Rev.*, 2010, **110**, 268–320.
19 P. Novák, K. Müller, K. S. V. Santhanam and O. Haas, *Chem. Rev.*, 1997, **97**, 207–282.
20 Y. G. Wang, H. Q. Li and Y. Y. Xia, *Adv. Mater.*, 2006, **18**, 2619–2623.
21 G. A. Snook, P. Kao and A. S. Best, *J. Power Sources*, 2011, **196**, 1–12.
22 Z. Chen and J. R. Dahn, *J. Electrochem. Soc.*, 2002, **149**, A1184.
23 Y. H. Huang, K. S. Park and J. B. Goodenough, *J. Electrochem. Soc.*, 2006, **153**, A2282.
24 I. Boyano, J. A. Blazquez, I. de Meatza, M. Bengoechea, O. Miguel, H. Grande, Y. Huang and J. B. Goodenough, *J. Power Sources*, 2010, **195**, 5351–5359.
25 H. R. Jung and W. J. Lee, *Solid State Ionics*, 2011, **187**, 50–57.
26 H. J. Ahonen, J. Lukkari and J. Kankare, *Macromolecules*, 2000, **33**, 6787–6793.
27 Q. Pei, G. Zuccarello, M. Ahlskogt and O. Ingan, *Polymer*, 1994, **35**, 1347–1351.
28 X. H. Liu, H. Zheng and L. Zhong, *et al.*, *Nano Lett.*, 2011, **11**, 3312–3318.
29 I. Ryu, J. W. Choi, Y. Cui and W. D. Nix, *J. Mech. Phys. Solids*, 2011, **59**, 1717–1730.
30 L. Hu, H. Wu, Y. Gao, A. Cao, H. Li, J. McDonough, X. Xie, M. Zhou and Y. Cui, *Adv. Energy Mater.*, 2011, **1**, 523–527.

 